E. E. Zukoski
J. M. Auerbach

California Institute of Technology, Pasadena, Ca.

Experiments Concerning the Response of Supersonic Nozzles to Fluctuating Inlet Conditions

The noise field produced by the passage of pressure and entropy fluctuations through a supersonic nozzle has been investigated in an experimental program. Magnitude and phase information for the disturbances produced within the nozzle are presented and are compared with numerical calculations.

Introduction

When a region of nonuniform enthalpy ("entropy spot," s') is convected through a steady flow field where the mean properties change rapidly along the flow direction (such as the velocity gradient dU/dx), an acoustic source results which is of the order $(dU/dx)^2(s'/C_p)$. Candel[1] and Marble[2] give some detailed analysis of such sources resulting from the passage of thermal nonuniformities through nozzles. Here, the strong field gradient (dU/dx or dP/dx) is provided by the nozzle contour.

Such sources are of particular importance in connection with combustion systems which invariably lead to nonuniform temperatures and consequent entropy fluctuations. A rather clear-cut example is the large scale fluctuation of temperature produced in an afterburner upstream of a choked nozzle. Estimates based on a compact nozzle approximation[2] show that when the nozzle is choked, the pressure fluctuation p' at the outlet, where the undisturbed pressure is p_2, gives the result that $p'/\gamma p_2 = \frac{1}{2}(M_1 + M_2) \cdot \frac{1}{2}(T'/T_1)$, where $\frac{1}{2}(M_1 + M_2)$ is the mean of the approach and discharge Mach numbers of the nozzle and T'/T_1 is the (random) fractional temperature fluctuation introduced by the combustion process ahead of the nozzle. The values T'/T_1 from 0.05 to 0.20, which are known to exist in both main burners and afterburners, thus lead to pressure fluctuations of a significant fraction of an atmosphere and, as a consequence, constitute a possible significant noise source.

A very similar and probably even more important situation occurs when the temperature fluctuations from the mean burner pass through the choked turbine nozzles. This source exists in the core engine of a high bypass ratio fan and consequently may be a dominant source of "excess noise" when the jet Mach number is low. When and if jet noise can be reduced, this internal noise source may become the dominant sound abatement problem for jet engines.

An experimental investigation has been initiated at Caltech with the financial support of the Office of Noise Abatement, Department of Transportation, to demonstrate the magnitude of these strong disturbances and to observe their actual strength in comparison with the results of extensive linearized analyses. In addition, it will be attempted to make measurements in the more complex case where the temperature disturbances approach the nozzle in a random fashion rather than as plane harmonic waves.

In the present paper we shall describe the experimental apparatus built for this investigation and the results of preliminary calculations and experiments.

Experimental Apparatus

The experimental apparatus to be used in the experimental program is described briefly in the following paragraphs. It has been constructed and is now in operation.

Gas Supply. The gas supply system, shown schematically in Fig. 1, was designed to maintain a flow of about one half kilogram per second to the test nozzle at a total pressure of 3 atm and at a low turbulence level. Nitrogen gas is drawn from 20 high-pressure gas bottles which have an initial pressure of 170 atm and a total capacity of 190 kg. A total operating time of about 100 s can be obtained with a single set of bottles. Operating procedures and quick-acting valves allow data to be taken over periods as short as 10–20 s.

[1] Candel, S., "Analytical Studies of Some Acoustic Problems of Jet Engines," PhD thesis, California Institute of Technology, Dec. 1971.

[2] Marble, F. E., "Acoustic Disturbance From Gas Nonuniformities Convected Through a Nozzle," *Proceedings, Interagency Symposium on University Research in Transportation Noise*, Vol. II, Stanford University, Calif., Mar. 28–30, 1973.

Contributed by the Gas Turbine Division and presented at the Gas Turbine Conference, Houston, Texas, March 2–6, 1975, of THE AMERICAN SOCIETY OF MECHANICAL ENGINEERS. Manuscript received at ASME headquarters December 2, 1974. Paper No. 75-GT-40.

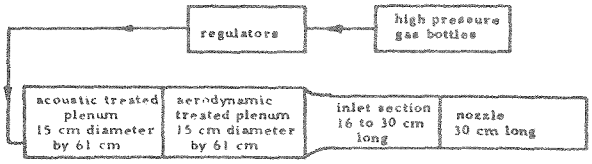

Fig. 1 Schematic diagram of flow system

Two dome-type regulators operating in series are used to hold the gas pressure constant during a run. They can be preset prior to the start of gas flow. Upstream of the nozzle and inlet sections, the gas first passes through a plenum chamber filled with Fiberglas which was designed to reduce reflections. The second section of the plenum chamber contains four 44-mesh screens and a 15-cm long section of straws designed to reduce the turbulence level of the flow. The Mach number in this section is nominally 0.02.

After traversing a contraction, the gas passes into the inlet section, which has a cross section of 2.5 × 7.6 cm and which contains the heater and mass bleed equipment discussed in the following. The Mach number in this section is 0.20.

Nozzle. The supersonic nozzle section which follows next is rectangular in cross section. It is 30 cm long and the 2.5 × 2.5 cm cross-sectional throat is located 20 cm from the inlet section. The nozzle currently in use has a nearly constant Mach number gradient of about 0.04 cm^{-1} and a less constant velocity gradient of about 100 s^{-1}. Measurements of the mean static pressure field in the nozzle have shown that the Mach number distribution is at all points within a few percent of the design linear distribution. Nozzle exit Mach number is 1.4.

Anechoic Chamber. The supersonic nozzle exhaust lies at the center face of an anechoic chamber which is cubic and has interior side dimensions of 300 cm. The interior surface consists of fiberglas wedges which produce free space conditions within ±2 db inside the chamber for frequencies greater than 300 Hz. A photograph taken during the construction of this chamber, Fig. 2*(a)*, illustrates the metal structure used to support the wedges. Test data indicate that the chamber operates satisfactorily for frequencies greater than 250 Hz. Typical data on sound pressure level are shown in Fig. 2*(b)*, where the sound pressure level measured on the axis of a speaker decays with the distance from the speaker, as required by free field theory. Agreement with free space field theory is within 2 db over the whole range of axial distances except for the 200 Hz signal.

Mass flow entering the chamber from the nozzle is exhausted from a 30 × 30 cm cross-sectional acoustically-treated duct placed at the center of the opposite wall.

Pressure Measurements. Mean static pressures were measured in the nozzle at 6 cm intervals with a strain gauge pressure-measuring instrument. Pressure fluctuations are measured at 6 stations at intervals of about 7.5 cm with high-frequency response piezoelectric gauges. Three similar stations are located in the inlet section and 3 others in the plenum section. Pressure fluctuation measurements in the anechoic chamber are made with B & K capacitance-type microphones.

Heater. The heater is made up of an array of 375 nichrome wires which are periodically heated by an electric current applied in the form of a square pulse wave train. The wires have a diameter of 0.010 cm and a length of 6.4 cm. Twenty-five of these wires are wound across two conductors 0.16 cm in diameter, which are supported by a rectangular frame made from a phenolic plastic about 0.32 cm thick. The inside edges of this frame form the 2.5 × 7.6 cm cross-sectional dimensions of the inlet section duct. Fifteen of these frames are stacked up to form the complete heater. A single frame and the fifteen-frame stack are shown in the photograph of Fig. 3. The wires in each frame are in parallel electrically and the frames are in series.

The electric current supply for the heater is drawn from a 0–300 V, 0–100 amp d-c power supply. Two silicon controlled rectifiers (SCR's) switch the large current flow to generate a square wave current pulse train which drives the heater. The duty cycle can be varied from 20–100 percent and the frequency from 200–1200 Hz.

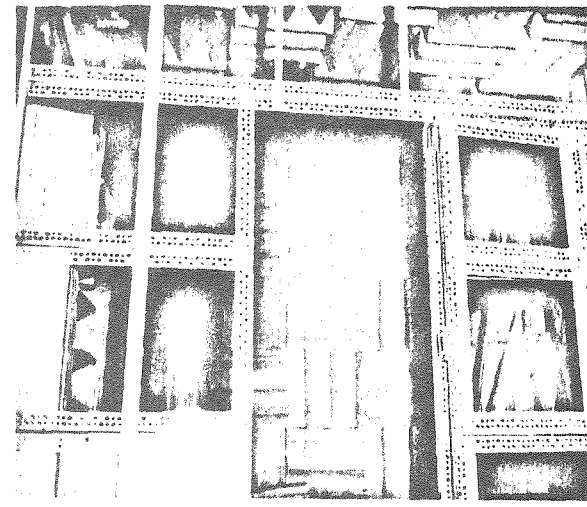

Fig. 2*(a)* Photograph of anechoic chamber illustrating construction details

The frequency can be controlled by either of the two techniques illustrated schematically in Fig. 4. When the heater is operated alone, the SCR switch system is driven by a pulse generator set at the desired frequency. When both heater and bleed valve systems are acting simultaneously (the situation illustrated in Fig. 4), we need to control the phase difference between the heater pulse and the valve position. This is done by directly measuring the valve position (photoelectrically) and using this signal in conjunction with a variable time delay or phase control system to set the phase of the SCR switch system.

A fluctuating temperature of about a degree centigrade can be produced in the 0.5 kg/s air flow with the heater system. The magnitude of this fluctuation is measured with a conventional constant-current hot wire anemometer set and a 0.001 cm dia wire with a frequency response several orders of magnitude above the heater operating frequency.

Bleed Valve. Mass is bled from the inlet section through one wall of the heater. The heater frames, described above and shown in Fig. 3, are separated by about 0.0125 cm to make flow passages 0.0125 × 6.0 cm in cross section between each frame. Sixteen of these passages in one side wall of the heater allow gas to pass into a shallow plenum chamber and on through a valve formed by a hole in a 1.25 cm rotating shaft. The mass flow rate is fixed by placing various calibrated orifices in the line downstream of the valve. The

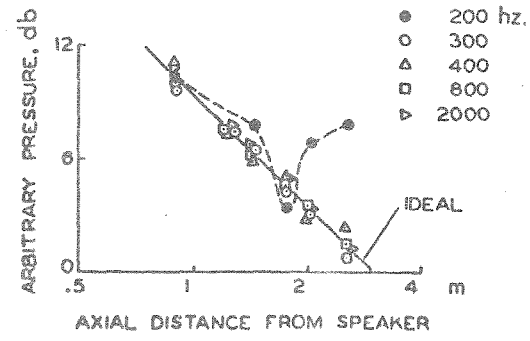

Fig. 2*(b)* Calibration data for anechoic chamber

shaft in the valve is rotated by a synchronous motor which is driven by a signal generator and power amplifier, as shown in Fig. 4. Valve frequencies between 0 and 450 Hz can be obtained.

A photoelectric device is used in conjunction with an 0.032 cm hole through the shaft to determine the angular position of the shaft. The phase difference between the shaft position and the initiation of mass flow from the inlet duct was determined by monitoring the gas flow out of one of the bleed passages in the heater wall with a hot-wire anemometer. Given this phase difference, the phase control system shown in Fig. 4 can be adjusted to fix the phase between heat addition and mass bleed as desired.

This system was developed so that the pressure signals generated at the heater, by the heat addition process, could be cancelled out or modified by periodically bleeding off gas with the appropriate frequency, phase and amplitude. Thus, the heater, when properly "compensated" in this manner, can be made to act as a pure source of entropy fluctuations. This technique has been successfully applied in the experiments discussed below.

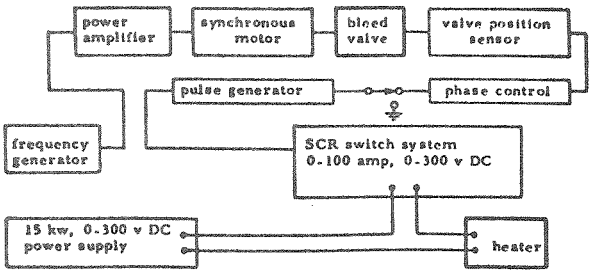

Fig. 4 Schematic of heater and bleed valve control system

Data Acquisition and Processing

The pressure and temperature fluctuations introduced by the heater and bleed systems upstream of the nozzle are of the order of 1 to 1/100 percent of the mean values of pressure and temperature. These relatively weak input signals produce pressure fluctuations in the duct which are of the order of 2×10^{-4} atm. Because the background aerodynamic noise in the duct is of roughly the same magnitude, signal processing is required to extract useful information.

Data Acquisition. Data are acquired from a variety of transducers as voltages, which are amplified to ensure that the signals of interest lie in the range between 10 V and 10 mV. Using the Hewlett-Packard 2100 Data Acquisition System, the signals are converted to digital values and are stored on a magnetic disc by the process shown schematically in Fig. 5. Data in digital form are acquired by this system at a rate of 60,000 words per s. Because only a single disk writing head is available, data can only be taken continuously for about 0.1 s when the 60,000 sampling rate is used. This presents a difficulty, because long sampling periods are needed to increase the signal-to-noise ratio of our data.

This difficulty is overcome and ease in processing the data is increased by using a phase lock acquisition technique. Data acquisition is started when the logic circuit, Fig. 5, simultaneously receives an "on" signal from the clock and a particular phase signal pulse from the heater or bleed valve input signal. Data acquisition terminates after about 0.10 s when the data buffer region of the computer core storage is filled with data. Each segment of data obtained in this manner starts with the same phase with respect to the input or forcing signal.

This arrangement allows the signals to be phase averaged. In this process the signals obtained from a large number of data samples and at a particular time after initiation of each data acquisition cycle are averaged. These average values are assembled for each sampling time to form a new signal which is one data segment long. The averaging process results in an increase in the amplitude of the signal in which we are interested (i.e., the signal produced by the response of the nozzle and supply system to the input signals), and a smaller increase in the noise. Because the signal of interest will increase linearly as the number of data segments is increased, and the noise will increase only as $\sqrt{N}$ (if it has a Gaussian distribution), a gain proportional to $\sqrt{N}$ is made in signal-to-noise ratio. In the present work, values of N between 60 and 150 are being used. Hence, a substantial gain can be made in signal-to-noise ratio.

The power of this process can be seen by comparing the two frequency spectra shown in Fig. 6. The lower section was obtained from a single data segment 0.10 s long. The upper spectrum is obtained from data obtained during the same experiment after averaging 100 data segments as outlined in the foregoing. In this example, the response to a heater input signal is shown. Background noise was found to behave as if it had a Gaussian distribution.

The outputs of 6 transducers are measured during a typical experiment, and each transducer output is sampled at 10 k Hz. This rate gives us 25 samples per transducer per cycle for a 400 Hz wave and is much more than required to define the wave unambiguously.

Typically, three channels are used to measure fluctuating pressures in the nozzle or inlet sections, one to measure temperature fluctuations produced by the heater, and the last two either for microphone measurements in the anechoic chamber or for measurements of mean flow quantities in the inlet section.

Data Processing. Data averaged by the technique described

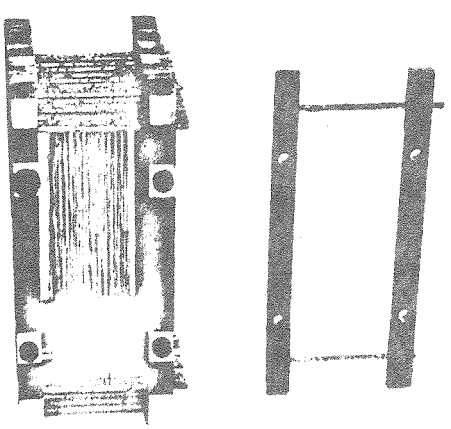

Fig. 3 Photograph of complete heater section and one heater frame

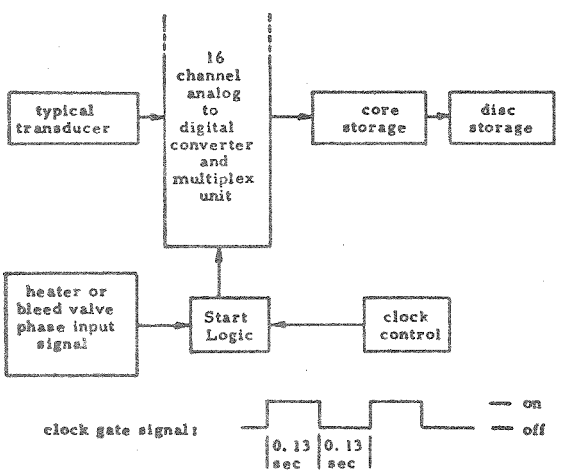

Fig. 5 Schematic of data acquisition system

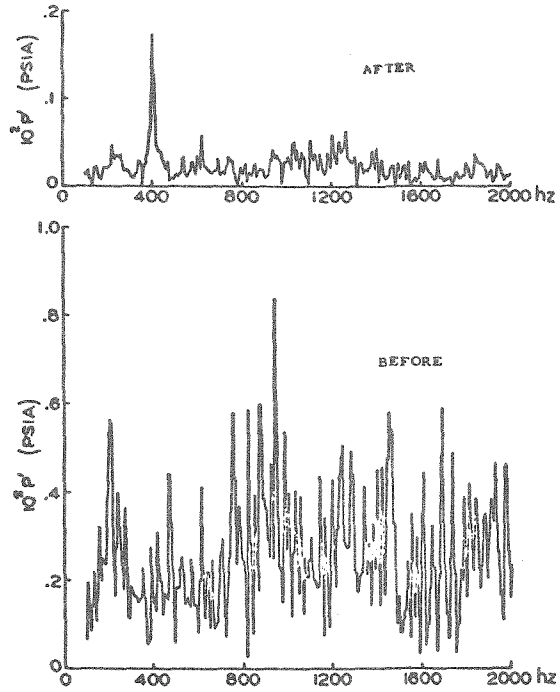

Fig. 6 Typical spectra before (lower) and after (upper) signal averaging

above have been processed on a digital computer by a Fourier transform technique to obtain spectra of the pressure signals similar to those shown in Fig. 6. This analysis yields both the magnitude and phase of the pressure signals induced by the input signals with a frequency resolution of about 10 Hz. Under certain circumstances, harmonics of the forcing frequency are set up and we can measure the response of the nozzle to input signals at a number of frequencies during the same experiment. Cross-correlation programs have been developed and used to examine the relationship between signals produced in the nozzle and in the anechoic chamber.

In addition to the measurements obtained by this technique, phase relations between various transducer signals can be obtained. For example, measurements made at two positions 15 cm apart in the constant-area inlet duct can be used to obtain amplitude and phase of the downstream running wave and the upstream or reflected wave. This information is being used to connect calculated and measured fluctuation amplitudes for the nozzle. Similar

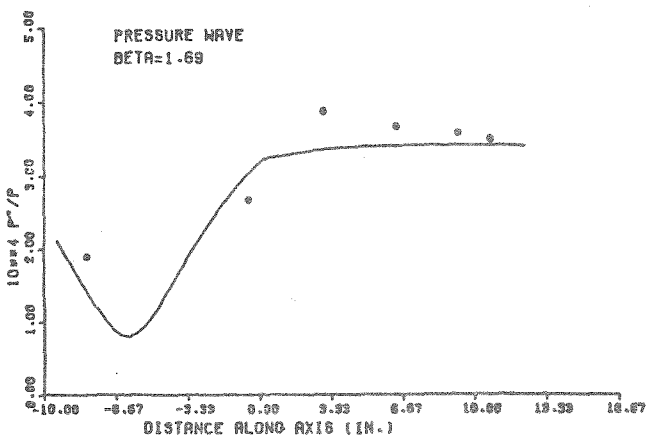

Fig. 7 Pressure fluctuation amplitudes due to mass bleed

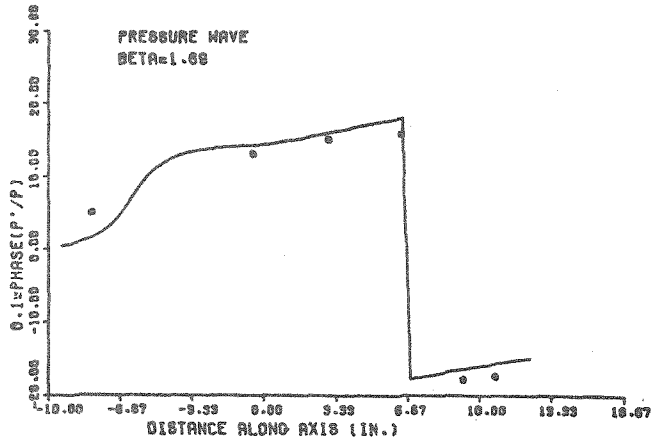

Fig. 8 Phase of pressure fluctuations of Fig. 7

data obtained from microphones will be used to examine the nature of the far field signal set up by the fluctuating signal leaving the nozzle exit.

Calculation

An analysis has been made of acoustic propagation through a one-dimensional duct of varying cross-sectional area which contains a mean flow and periodic sources of heat and mass. The equations of motion are solved numerically for the mean flow through the duct for given cross-sectional area variation under the assumption that the flow is isentropic. The equations are also linearized for the study of small flow perturbations about the mean flow due to heat and mass addition.

The energy equation for the perturbation quantities is not coupled to the continuity and momentum equations. It can be solved independently and used to match arbitrary input functions for heat addition. Manipulation of equations of continuity, momentum, and state leads to a pair of coupled linear ordinary differential equations for the pressure and velocity perturbation fields.

The duct geometries investigated simulate the supply system starting at the plenum chamber, the inlet sections, the heater and bleed systems, and the supersonic nozzle used in the experiments. Solutions were obtained by numerical integration of the equations. Because the equations have a singularity at the throat, the numerical integration is started there and proceeds both up and down stream.

When the forcing function is a simple mass bleed, an upstream

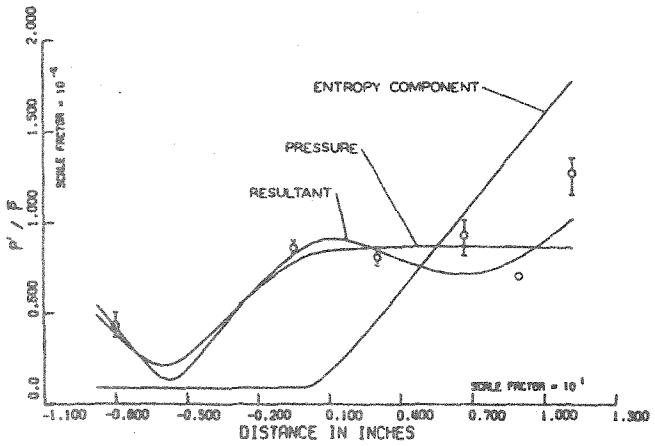

Fig. 9 Pressure fluctuation amplitudes due to the uncompensated heater

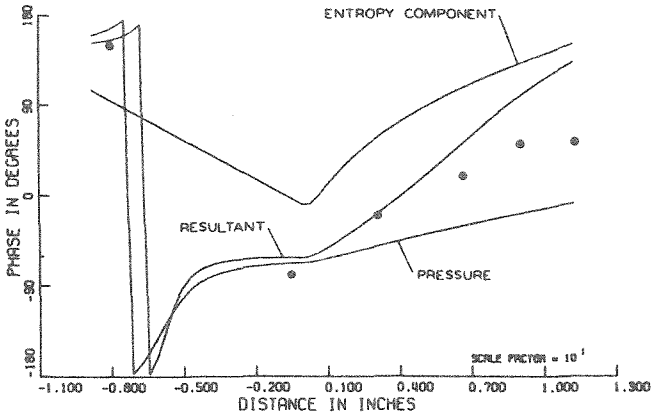

Fig. 10 Phase of pressure fluctuations of Fig. 7

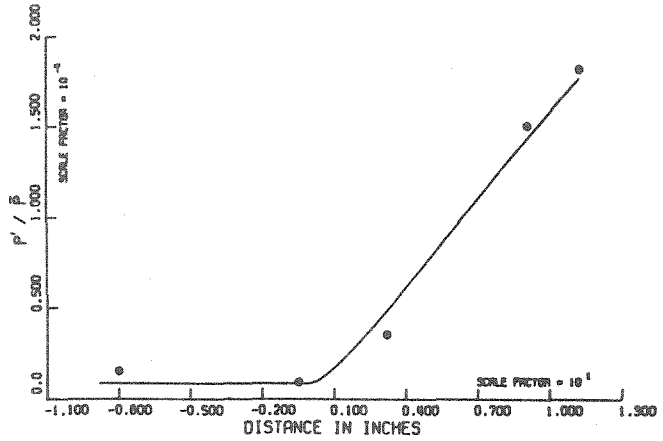

Fig. 11 Pressure fluctuation amplitudes due to compensated heater

matching condition is specified either as a pressure at some point upstream or as an incident pressure wave at the nozzle entrance. In the latter case, the incident wave is obtained from the experimental determination of both incident and reflected waves. Given the determination of the subsonic solutions, the calculation can then be continued into the supersonic section of the nozzle.

A similar solution could be carried out for the case of a simultaneous heat and mass bleed. Entropy fluctuations are measured at the nozzle inlet and a solution of the entropy field is then obtained. Again, two pressure measurements are made in a straight section upstream of the nozzle entrance and a matching condition is calculated. The equations are solved using the matching condition to give a general solution from a homogeneous solution (no entropy fluctuation) and a nonhomogeneous solution.

Solutions have been obtained for a range of geometric configurations, upstream matching conditions, and heat addition and mass bleed values. Typical results are given in Figs. 7–11, which are discussed in the following section.

Results

The response of the system to a 400 Hz signal produced by the mass bleed system is shown in Figs. 7 and 8. Similar data are shown for the response to the heater operating alone in Figs. 9 and 10, and for the "compensated" heater case in Fig. 11. In all of these examples, the heater and bleed valve are located at −9 in. in a constant-area duct which extends downstream to the nozzle entrance at the 0.0-in. location. The nozzle throat lies at the 7.5-in. station and the measured exit Mach number is 1.4. Here, P' is the magnitude of the fluctuation, and $\bar{P}$ is the local average static pressure.

When the heater is operating alone, it produces the desired entropy fluctuation, but in addition produces a pressure fluctuation due to the local change in density of the periodically heated gas. These two fluctuations, the convected entropy wave and the propagating pressure signal, interact as they pass through the nozzle to produce a complicated spatial distribution of amplitude and phase. The data and calculated values shown in Figs. 9 and 10 illustrate this point.

The theoretical curve labeled "pressure" in Fig. 9 represents the calculated amplitude of the pressure-induced signal and consequently has the same shape as that shown in Fig. 7 for the pure pressure wave. Similarly, the magnitude of the entropy-induced signal, "entropy component" in Fig. 9, has the same shape as that for the compensated heater case shown in Fig. 11. The "resultant" shown in Fig. 9 is the magnitude of the vector sum of the two components.

The results of using the compensation technique described in the foregoing are shown in Fig. 11. Here, the amplitude of the pressure signal produced by the heater operated with appropriate compensation is shown for a 400 Hz heater signal. Agreement between theory and experiment is excellent, and it is clear that a "compensation" process can be used to reduce the pressure fluctuation produced by the heater to negligible values.

In making the calculations shown in Figs. 7–11, experimental values of the pressure fluctuation amplitude and phase measured in the straight section upstream of the nozzle, at −8 and −0.5 in. stations, and the measured temperature fluctuations at station −0.5, were used as boundary conditions. The data are average values for 3 runs, and they agree well with the calculations.

Data similar to that shown here have been obtained for the frequency range $450 \geq f \geq 250$ Hz, and the agreement between calculated and theoretical values was comparable to that shown here.

The nozzle entrance position in these plots is at 0.0, and it is clear that the pure pressure and entropy components of the pressure disturbance have a radically different character in the nozzle. The magnitude (and to a lesser extent the phase) of the pure pressure component is almost constant throughout the nozzle. In contrast, the entropy component grows almost linearly from the nozzle inlet to the exit plane, and its phase change is also large.

These results were obtained for a frequency f of 400 Hz and a reduced frequency fL/a^* of 1.69, where L is the subsonic nozzle length and a^* is the velocity of sound at the throat. In terms of the nozzle exit reduced frequency, fd/u_{exit}, the value is about 0.03. However, calculations carried out for frequencies between 0 and 4000 Hz for this system showed a similar type of distribution for both pure pressure and entropy disturbances incident on the nozzle.

It is interesting to estimate the magnitude of the *internal* acoustic field set up by heat addition fluctuations in a turbojet primary burner or afterburner. In the absence of any local resonance or strong interactions between acoustic field and burner instability, temperature fluctuations of the order of 10 percent are reasonable. If the data of Fig. 9 are scaled up linearly to this level, a change by a factor of 50 to 100, one could expect pressure fluctuations of the order of 1 percent of the local static pressure throughout the nozzle.

The results described in the foregoing show that the internal acoustic field set up by the passage of plane pressure or entropy waves, or a combination of these, through a convergent-divergent supersonic nozzle is well understood, both theoretically and for this particular experimental apparatus. Thus, the apparatus has been shown to be a reliable tool for the study of more complex disturbances for which calculations are not available. We are currently studying two of these: first, the noise produced by two-dimensional rather than plane entropy patterns; and second, the noise field produced outside the nozzle, in the far field of the jet, by pressure and entropy waves incident on the nozzle inlet.